Journal Name

ARTICLE TYPE

Cite this: DOI: 10.1039/xxxxxxxxxx

Gate-Controlled Heat Generation in ZnO Nanowires FETs †

Andrea Pescaglini,[a] Subhajit Biswas,[b,c] Davide Cammi,[d] Carsten Ronning,[d] Justin D. Holmes,[b,c] and Daniela Iacopino[a]

1 Supplementary material

1.1 Optimization of the metal contacts

In order to investigate the electronic properties of ZnO nanowires, a reliable method to form ohmic metal-ZnO contact is strictly required. Addressing this aspect is not only crucial for studying the electronic properties of the nanowire but also for the performance of the FET device described in the article.

Figure 1a compares the two-terminal I-V characteristics of a NW-FET device with Ti(90 nm)/Au(50 nm) (black line) metal contacts and a device with Ti(10 nm)/Al(90 nm)(blue line). The resistance of the device with Ti/Au pads was larger than 10^9 Ω and the non-linear I-V curve (see inset of figure 1a) was indicative of a non-Ohmic contact between the metal and the nanowire. In order to demonstrate that the high resistance was related to the contact resistance, we compared this result with the I-V curve measured in a device with Ti/Al contacts. For Al contacts the I-V response was clearly linear (ohmic contacts) and the resistance was of the order of 10^5-10^6 Ω, more than three orders of magnitude lower than the resistance observed in the previous device (Au). The observed behavior can be explained from the energy band structure alignment. The work-function of Au (5.47 eV) is higher than the work function of ZnO (4.65 eV).[1] At the metal-nanowire interface the electron depletion inside the ZnO results in upward band bending and formation of a Schottky barrier, giving rise to high contact resistance and non-ohmic behaviour. On the other hand, the lower work-function of Al (4.33 eV) induces a downward band bending in the ZnO and consequently an ohmic response. These results show that the contact resistance can be reduced by at least 3 orders of magnitude with Al electrodes, thus allowing a more efficient electron injection and collection than Au. It is worth to notice that although the Al does oxidise in air, the thin oxide layer (1-2 nm) was mechanically removed by direct probing. Therefore it did not affect the electrical characterization of the devices.

The effect of thermal annealing on the Ti/Al contact resistance was also investigated. The device was heated up with a rate of 2 °C/s to 300 °C and annealed for 5 min in forming gas. Figure 1b shows the I-V curves recorded before and after two annealing processes. A reproducible trend was observed in 5 devices: the resistivity was reduced by more than one order of magnitude (figure 1c). The lowering of contact resistance after annealing was previously explained by Kim *et al.*.[2] The formation of TiO species and the related oxygen vacancies V_O form shallow donors near the conduction band with consequent electron enrichment. It should be noticed that in our experiments this trend was not confirmed over different batches of ZnO nanowires and an increasing of the device resistance of 1-2 orders of magnitude was also observed after the annealing process under comparable conditions. However, for those devices the two-terminal resistance without annealing was already in the range of 10^5-10^6 Ω, comparable with the valued obtained in the devices showed in figure 1c after two consecutive annealing processes. ZnO NW-FETs discussed in the article were fabricated with Ti/Al electrodes without any annealing process.

Figure 1d-f show the resistance values in various atmospheres. The conductivity of ZnO nanowires was found larger in high vacuum compared to air as shown the I-V curve of figure 1d. Statistics performed on 9 devices showed that the nanowire resistance in high vacuum was lower than in air by more than one order of magnitude. This variation is due to the presence of electron traps created by oxygen species adsorbed on the nanowire surface that reduced the free electrons available for conduction.[3]

1.2 Electrical characterization

We provide an estimation of the contact resistance by measuring the I-V_g curve of the NW-FET device (Figure 2a-b) and using the approximated current equation in the linear regime ($V_D \ll V_g$)[4]

[a] *Tyndall National Institute, Dyke Parade, Cork, Ireland. E-mail: andrea.pescaglini@tyndall.ie*
[b] *Department of Chemistry and Tyndall National Institute, University College Cork, Cork, Ireland.*
[c] *AMBER@CRANN, Trinity College Dublin, Dublin 2, Ireland.*
[d] *Institute of Solid State Physics, Friedrich-Schiller-University of Jena, Max-Wien-Platz 1, 07743 Jena, Germany.*

† Electronic Supplementary Information (ESI) available: [details of any supplementary information available should be included here]. See DOI: 10.1039/b000000x/

‡ Additional footnotes to the title and authors can be included *e.g.* 'Present address:' or 'These authors contributed equally to this work' as above using the symbols: ‡, §, and ¶. Please place the appropriate symbol next to the author's name and include a `\footnotetext` entry in the the correct place in the list.

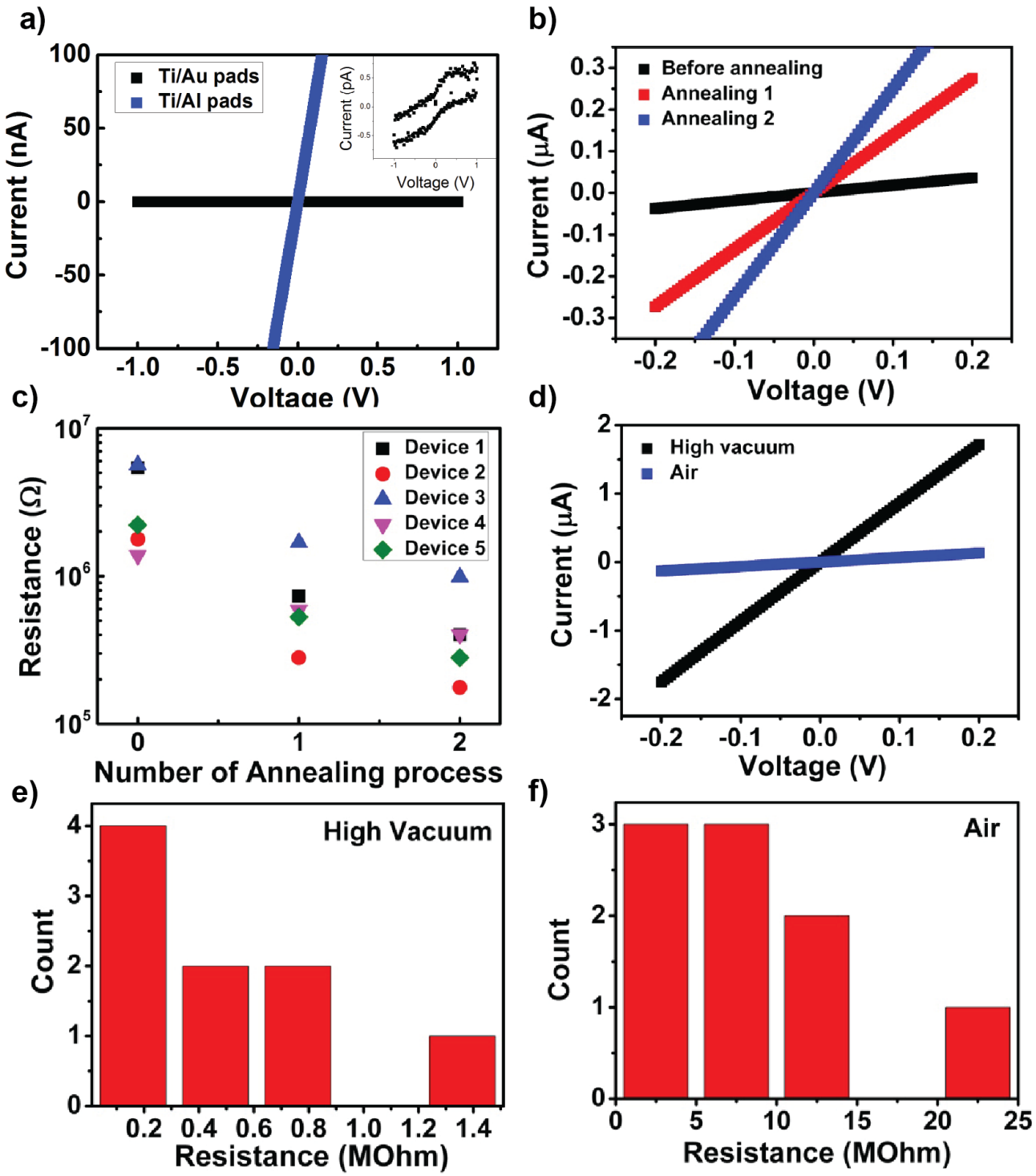

Fig. 1 a) I-V characteristic in air of a ZnO nanowire contacted with Ti/Au (90 nm/50 nm) and Ti/Al (10 nm/90 nm) pads separated by 2 μm. b) I-V characteristic of a ZnO nanowire contacted with Ti/Al/Ti (10 nm/150 nm/50 nm) electrodes before and after two annealing processes. c) Resistance measured in two-terminal configuration for 5 devices before and after two annealing processes. d) I-V characteristic of ZnO nanowire with Ti/Al (10 nm/90 nm) pads separated by 2 μm in air and in vacuum. Statistical distribution of the resistance from 9 devices with Ti/Al (10 nm/90 nm) pads in e) high vacuum and f) in air.

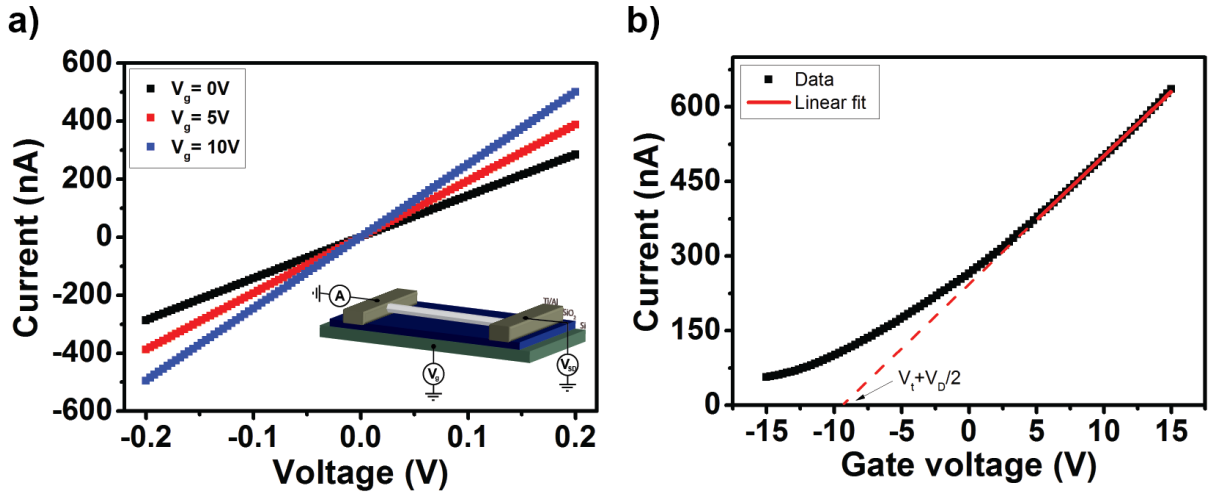

Fig. 2 *a) I-V characteristic with different gate voltages applied and b) the I-V_g curve of a NW-FET in air.*

$$\begin{cases} \frac{dI_{SD}}{dV_D} = \frac{\mu C_{NW-gate}}{L^2}(V_g - V_t) \\ \frac{dI_{SD}}{dV_g} = \frac{\mu C_{NW-gate}}{L^2} V_D \end{cases} \quad (1)$$

where I_{SD} is the source-drain current, V_D and V_g is the drain and back-gate voltage respectively, L the channel length and $C_{NW-gate}$ is the gate-capacitance expressed by

$$C_{NW-gate} = \frac{2\pi\varepsilon_0\varepsilon_r L}{cosh^{-1}\left(\frac{r+h}{r}\right)} \quad (2)$$

where h is the SiO_2 thickness and r the nanowire radius and ε_r=3.9 the dielectric constant of the SiO_2. This analytical expression holds for cylindrical nanowires completely embedded in SiO_2, however finite-element simulations showed that eq.(2) over-estimate the capacitance by only a factor ~2, thus still providing the correct order of magnitude.[5] The I-V_g curve (figure 2b) indicates an evident n-type conduction in the ZnO nanowires. The threshold voltage V_t was calculated by direct extrapolation, as shown in figure 2b, where the value on the V_g axes is the quantity $V_t + \frac{V_D}{2}$. For the device shown in figure 2 we obtained V_t=-9.39±0.08 V. The negative V_t value suggests the presence of unintentional *n*-type. However, due to the variability of the nanowire diameters within the as-grown batch and the depletion of free electrons by the oxygen species adsorbed on the surface in air, the V_t values in the measured NW-FETs were found variable in the range of -10/10 V. Using V_t and the transconductance (dI_{SD}/dV_g) calculated in the linear region (for V_g > 5 V) was possible to obtain the channel conductance by using

$$R_{FET} \equiv \frac{dI_{SD}}{dV_D} = \frac{dI_{SD}}{dV_g}\frac{V_g - V_t}{V_D} \quad (3)$$

In table 1 we compare the measured resistance R_m in two-terminal configuration and the resistance R_{FET} calculated from equation 3 for different applied gate voltages.

The calculated and measured values were reasonably close, in particularly the discrepancy decrease for larger back-gate voltage and at V_g=10 V the R_m and R_{FET} were coincident within the error. In fact, since the linear fit was calculated for V_g>5 V, eq.(1) performs better in that range. Nevertheless, the excellent agreement between the channel resistance R_{FET} and the two-terminal resistance R_m demonstrates that the contact resistance is effectively negligible compared to the channel resistivity, and by direct comparison, was estimated on the order of $R_c \sim 10^3$ Ω or lower. We emphasize that this is a rough estimation and a more precise analysis would require four-terminal measurements on a single nanowire. However, from R_c we calculated the contact resistivity ρ_c by using the formula[6]

V_g (V)	R_m (Ω)	R_{FET} (Ω)
0	$7.007 \pm 0.002 \cdot 10^5$	$8.29 \pm 0.09 \cdot 10^5$
5	$5.1607 \pm 0.0005 \cdot 10^5$	$5.41 \pm 0.05 \cdot 10^5$
10	$4.0242 \pm 0.0009 \cdot 10^5$	$4.01 \pm 0.03 \cdot 10^5$

Table 1 *Resistance R_m of the representative device measured in two-point configuration compared with the resistance R_{FET} calculated using eq.3 when a back-gate voltage of 0, 5 and 10 V was applied.*

$$\rho_c = \frac{R_c^2 2\pi^2 r^3}{\rho_{NW}} \quad (4)$$

and a value of $10^{-11} - 10^{-10}$ Ω·m^2 with $R_c \sim 10^3 - 10^4$ Ω was obtained. Notably this estimation is in reasonable agreement with the reported value in literature for ZnO-Al contacts reported by Kim *et al.*.[2] Equation 4 is valid in the limit of long contacts $L \gg L_T$ where the transfer length L_T

$$L_T = \frac{\pi r^2 R_c}{\rho_{NW}} \quad (5)$$

was found in the range of $\sim 10 - 100$ nm using $R_c \sim 10^3 - 10^4$ Ω and $\rho_{NW} \sim 5 \cdot 10^{-3}$ Ω·m. This is much smaller than the contact length of the two metal electrodes in the measured device that

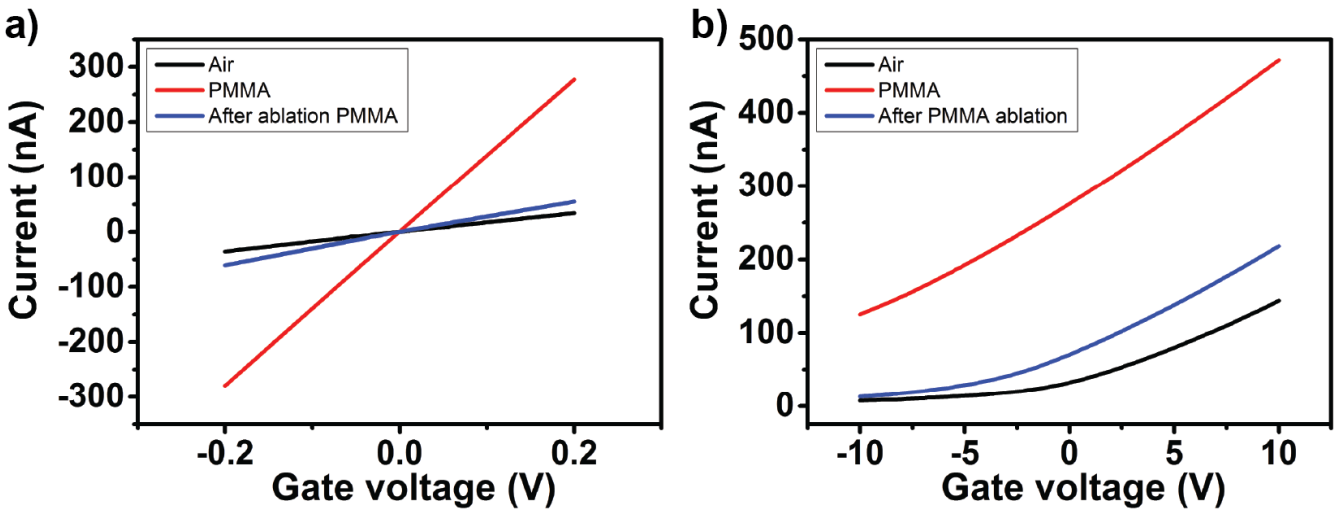

Fig. 3 *a) I-V characteristic of a representative device in air, covered by PMMA and after the ablation process. b) I-V_g characteristic of the device in air, covered by PMMA and after the ablation process.*

was 4.7 μm and 8.5 μm, respectively, thus justifying the use of eq.(4).

A number of physical parameters were extracted by further analysis. The electron mobility was calculated by using

$$\mu = \left|\frac{dI}{dV_g}\right|_{V_D} \cdot \frac{L^2}{C_{NW} \cdot V_D}. \quad (6)$$

The calculated field-effect mobility was estimated to be 58 $cm^2/V{\cdot}s$ in agreement with previous reports.[7] Carrier concentration was calculated using the Drude approximation by

$$n = \frac{1}{\mu e \rho} \quad (7)$$

with e the elementary charge and ρ_{NW} the nanowire resistivity. The carrier concentration was estimated to be 10^{17} cm^{-3}.

1.3 Electrical characterization before and after Joule heating process

The electrical properties of a representative ZnO NW-FET was monitored before and after the Joule heating process. Figure 4a-b compare the I-V and the transconductance of a NW-FET in air and covered by PMMA before ablation, and after the ablation process. In air, the nanowire resistance was $5.76 \pm 0.07 \cdot 10^6$ Ω (with V_g=0), the transconductance dI_{SD}/dV_g=1.27±0.01 10^{-8} S and the V_t=-1.07±0.02 V. When the nanowire was covered by PMMA the resistance, transconductance and threshold voltage became $7.187 \pm 0.001 \cdot 10^5$ Ω (with V_g=0), 1.962±0.006 10^{-8} S and the V_t=-13.81±0.06 V, respectively. Finally, after the ablation process, we found that the nanowire resistance was $3.45 \pm 0.07 \cdot 10^6$ Ω (with V_g=0), the transconductance dI_{SD}/dV_g=1.596±0.007 10^{-8} S and the V_t=-3.49±0.02 V.These values are very close to the resistance, transconductance and threshold voltage measured in air before ablation, demonstrating the PMMA removal during the Joule heating process.

References

1 S. Dhara and P. Giri, *Journal of Applied Physics*, 2011, **110**, 124317–9.

2 S. Young Kim, H. Won Jang, J. Kyu Kim, C. Min Jeon, W. Il Park, G.-C. Yi and J.-L. Lee, *Journal of Electronic Materials*, 2002, **31**, 868–871.

3 D. Cammi, *PhD thesis*, Physikalisch-Astronomischen Fakultat der Friedrich-Schiller-Universitat Jena, 2016.

4 S. M. Sze and K. K. Ng, *Physics of semiconductor devices*, John Wiley & Sons, 2006.

5 O. Wunnicke, *Applied Physics Letters*, 2006, **89**, 083102.

6 S. E. Mohney, Y. Wang, M. A. Cabassi, K. K. Lew, S. Dey, J. M. Redwing and T. S. Mayer, *Solid-State Electronics*, 2005, **49**, 227–232.

7 J. Goldberger, D. J. Sirbuly, M. Law and P. Yang, *The Journal of Physical Chemistry B*, 2005, **109**, 9–14.